

UCLA

UCLA Previously Published Works

Title

Frequency-Scanning Phased-Array Feed Network Based on Composite Right/Left-Handed Transmission Lines

Permalink

<https://escholarship.org/uc/item/4zc535q5>

Journal

IEEE Transactions on Microwave Theory and Techniques, 61(8)

ISSN

0018-9480

Authors

Choi, Jun H
Sun, Jim S
Itoh, Tatsuo

Publication Date

2013-08-01

DOI

10.1109/tmtt.2013.2263508

Peer reviewed

Frequency-Scanning Phased-Array Feed Network Based on Composite Right/Left-Handed Transmission Lines

Jun H. Choi, *Student Member, IEEE*, Jim S. Sun, *Student Member, IEEE*, and Tatsuo Itoh, *Life Fellow, IEEE*

Abstract—This paper presents an all-passive phased-array feed network based on composite right/left handed (CRLH) transmission lines (TLs). A CRLH TL enables systematic engineering of the phase response providing phase advance in addition to phase delay. When utilized in a phased-array feed network, an all-passive 1-D frequency-scanning array can be designed with a large scanning angle range toward both positive and negative elevation angles. This unique feature cannot be realized using conventional delay lines or dispersive lines that do not contain left-handed properties. Also, unlike the previously studied CRLH-based leaky-wave antennas that provide similar 1-D continuous frequency-scanning functionality, the proposed method completely decouples the radiating antenna element from the array factor; thereby providing extra design freedom and enhanced radiation performance. To validate the added advantage, we use the proposed CRLH-based phased-array feed network to demonstrate simultaneous controllability of the radiated polarization and array current amplitude distribution.

Index Terms—Antenna array, composite right/left-handed (CRLH), feed network, frequency scanning, phased array, quasi-Yagi antenna.

I. INTRODUCTION

COMPOSITE right/left-handed (CRLH) based frequency-scanning antennas have attracted much attention in recent years. Unlike the previous generation of frequency-scanning leaky-wave antennas (LWAs) that could only scan toward one direction with respect to broadside (excluding broadside radiation) [1], [2], the CRLH concept enable full frequency-scanning capability from backfire-to-endfire including broadside while operating in the dominant mode. Popular CRLH-based LWAs can be analyzed using antenna array theory [3]. The antenna is composed of periodic structures with unit dimensions much smaller than the guided wavelength. When the antenna is fed from one end of the leaky-wave mechanism, each antenna element contributes a small portion of the radiated power. Careful

design of the antenna structure essentially provides both negative and positive phase progressions between each unit element as frequency is varied within the radiating frequency band. Since the introduction of CRLH-based LWAs in 2002 [4], [5], researchers have focused on improving antenna functionalities and performances. For example, common and differential mode feeding is added to control and improve the radiated far-field polarization [6]. Amplifiers are inserted to control the amplitude distribution and increase the radiated gain toward broadside radiation [7]. Substrate integrated waveguide (SIW) is utilized to increase the quality factor (Q) of the antennas [8]. Despite each novel approach, CRLH-based LWAs have an inherent drawback that arises from closely coupled linkage between the radiating antenna elements and the array factor (AF). In order for CRLH LWAs to provide smooth frequency-scanning operation, a very specific structural form must be retained, but in doing so, independent control of the antenna parameters, such as polarization and amplitude distribution, are sacrificed.

This paper presents a different approach in designing a frequency-scanning radiating circuit. The proposed method also uses the CRLH concept, but rather than integrating the approach into the antennas, the phase engineering concept of the CRLH TL is applied to the phased-array feed network, which is completely decoupled from the radiating elements. In doing so, independent design controllability can be obtained to easily alter radiated polarization type, polarization orientation, and cross-polarization level. Furthermore, when combined with power dividers that allow simple power ratio adjustments, current amplitude distribution of the array can be easily manipulated to control the directivity and main-lobe level to SLL of the radiated pattern. To the authors' knowledge, an all-passive full frequency-scanning radiating circuit that allows independent controllability of polarization, phase, and amplitude distribution has not yet been demonstrated. To address the similarities and differences with the CRLH LWA, we present a brief review of the conventional CRLH LWA, followed by the new design approach for frequency-scanning arrays based on the CRLH transmission line (TL). Finally, the improved radiated performances of the proposed system are highlighted and validated with measured results.

II. CONVENTIONAL CRLH LWA

CRLH LWAs are composed of periodic unit cells containing reactive parameters that provide both negative and positive propagation constant (β) values as a function of scanned frequency. The equivalent-circuit model of the unit cell is shown

Manuscript received January 09, 2013; revised April 17, 2013; accepted April 22, 2013. Date of publication June 04, 2013; date of current version August 02, 2013.

The authors are with the Electrical Engineering Department, University of California at Los Angeles, Los Angeles, CA 90095 USA (e-mail: choijh@ucla.edu; b91901018@gmail.com; itoh@ee.ucla.edu).

Color versions of one or more of the figures in this paper are available online at <http://ieeexplore.ieee.org>.

Digital Object Identifier 10.1109/TMTT.2013.2263508

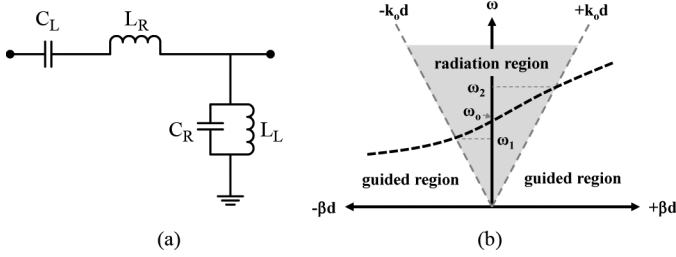


Fig. 1. CRLH unit-cell. (a) Equivalent-circuit model comprised of the left-hand and right-hand reactance values and (b) dispersion diagram.

in Fig. 1(a). For frequencies where $-k_o < \beta < +k_o$, the guided mode couples to air and radiates with a main beam at an angle

$$\theta_o = \sin^{-1} \left(\frac{\beta(\omega)}{k_o} \right) \quad (1)$$

where $\beta(\omega)$ is the frequency-dependent propagation constant and k_o is the free-space wavenumber. Under the balanced condition

$$Z_o = \sqrt{\frac{L_R}{C_R}} = \sqrt{\frac{L_L}{C_L}} \quad (2)$$

a smooth transition from backfire to endfire can be obtained without introducing the undesired bandgap frequency region [9]. A typical dispersion diagram of a balanced CRLH LWA is shown in Fig. 1(b). In sum, operating the CRLH structure between the radiation frequency region ($\omega_1 < \omega < \omega_2$), the structure behaves as an antenna with a main beam that scans along the elevation angles as the frequency is varied. However, most planar types of CRLH LWAs [10], [11] suffer from the difficulties in controlling radiated polarization characteristics and from the nonideal exponentially decaying amplitude distribution profile. For TL-based CRLH LWA structures, nonideal polarization traits have been remedied by combining a set of antennas side-by-side and feeding common/differential mode signals [6]. Different structural types such as the SIW have demonstrated relatively better polarization characteristics for a particular E -plane orientation [8]. However, in all cases, directivity/sidelobe level (SLL) controllability remains unresolved. To add the amplitude controllability and increase directivity, unidirectional amplifiers have been added to the CRLH LWA [7]. In doing so, tapered amplitude distribution has been provided for broadside radiation, but frequency-scanning capability has not been demonstrated. Also, integrating amplifiers adds both design and fabrication complexity, in addition to forfeiting bilateral (Tx. and Rx.) operation. However, to simultaneously address polarization and amplitude distribution properties, CRLH TLs may be used in the form of a phased-array feed network, as described in the following.

III. PHASED-ARRAY NETWORK BASED ON CRLH TLs

The essential property required in continuous frequency scanning is obtained by gradually increasing the relative phase pro-

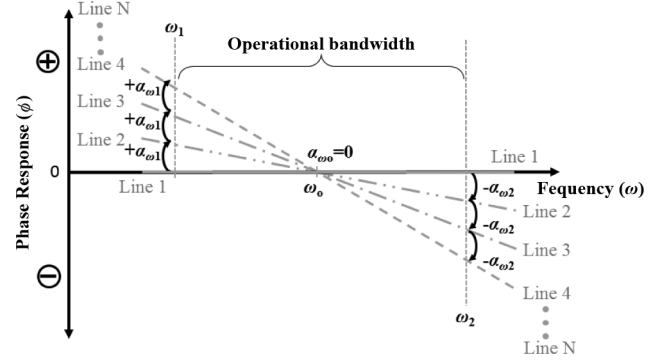


Fig. 2. Ideal phase response of four-element linear phased-array feed network needed for continuous 1-D frequency scanning.

gression between the antenna elements toward both negative and positive directions as frequency is shifted away from the center frequency ω_o (Fig. 2). The equation for the main beam angle describing the phased array has the same form as that of the CRLH LWA

$$\theta_o = \sin^{-1} \left(\frac{\alpha}{kd} \right). \quad (3)$$

Here, if the progressive phase shifting (α) between the antenna elements can be both negative/positive and dispersive [$\pm\alpha(\omega)$] for a fixed inter-element spacing (d), the same full 1-D frequency-scanning feature obtained in CRLH LWAs can also be achieved, but all in passive phased-array form. The above requirements can be satisfied using a nonradiating CRLH TL (realized using lumped components) based phased-array network. Unlike the conventional TLs, the CRLH TL allows simpler systematic manipulation of the phase response between the input and output ports of the line. The equivalent circuit model is the same as that of the CRLH LWA, but when lumped devices are used, radiation is suppressed. The phase response between the input and output ports of a given CRLH TL is a sum of the left-handed (LH) phase response and the right-handed (RH) phase response created by the constituent reactance values comprising the LH and RH portions of the CRLH TL as follows:

$$\phi_c = \phi_R + \phi_L \approx -n\omega\sqrt{L_R C_R} + \frac{n}{\omega\sqrt{L_L C_L}}. \quad (4)$$

The above concepts have been extensively researched in designing dual-band microwave circuits [12]–[14], but have not been applied for broadband frequency-scanning phased-array networks. In [15], brief introduction of the capability in utilizing CRLH lines as frequency-scanning phased-array feed network has been demonstrated. This paper is an expansion of [15], where a larger scanning angle is provided by eliminating the CRLH lines in one of the feeding path and also amplitude distribution is examined to demonstrate main-lobe-to-sidelobe controllability. Unlike [7], bilateral operation is allowed in this system since only passive elements are utilized to control the radiated parameters. A systematic approach of providing the de-

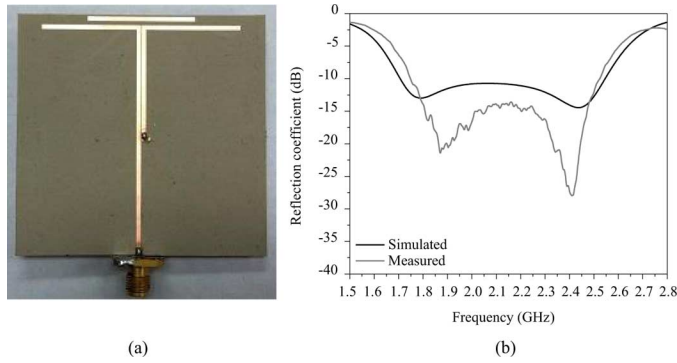


Fig. 3. *R*-band single element quasi-Yagi antenna. (a) Photograph of the fabricated antenna. (b) Simulated and measured reflection coefficient plots.

sired phase response for the two frequency points are shown in the following equations [9]:

$$\begin{aligned}
 L_R &= \frac{Z_o \left[\phi_1 \left(\frac{\omega_1}{\omega_2} \right) - \phi_2 \right]}{n\omega_2 \left[1 - \left(\frac{\omega_1}{\omega_2} \right)^2 \right]} \\
 C_R &= \frac{\phi_1 \left(\frac{\omega_1}{\omega_2} \right) - \phi_2}{n\omega_2 Z_o \left[1 - \left(\frac{\omega_1}{\omega_2} \right)^2 \right]} \\
 L_L &= \frac{nZ_o \left[1 - \left(\frac{\omega_1}{\omega_2} \right)^2 \right]}{\omega_1 \left[\phi_1 - \left(\frac{\omega_1}{\omega_2} \right) \phi_2 \right]} \\
 C_L &= \frac{n \left[1 - \left(\frac{\omega_1}{\omega_2} \right)^2 \right]}{\omega_1 Z_o \left[\phi_1 - \left(\frac{\omega_1}{\omega_2} \right) \phi_2 \right]} \quad (5)
 \end{aligned}$$

where n is the number of unit-cells and ϕ_1 and ϕ_2 are the desired phase values at frequencies ω_1 and ω_2 , respectively. With the proper reactance values, the zero phase-response point can be shifted from dc to an arbitrary frequency point (ω_o) and the phase slope can also be manipulated to adjust the desired phase values at the two far ends of the frequency points (ω_1 and ω_2). Although the phase response becomes nonlinear as the frequency moves away from the center point, sufficient linear response is observed for usable frequency band. Ultimately, for every added antenna element, the phase response of the CRLH lines should be designed so the phase difference ($\alpha_{-N} = \phi_{\text{line } N+1} - \phi_{\text{line } N}$) between every adjacent pair of feed lines are equal to each other at each frequency point within the operating frequency band. To obtain full 1-D frequency scanning, the final phase response should resemble Fig. 2. CRLH dispersive lines only contribute to the phase component of the array system. Slight amplitude perturbation may be created between the lines due to the lossy nature of lumped elements, but the amplitude imbalance can be easily compensated by adding an unequal power divider in the first power division step. This technique is applied in the fabricated circuits, as will be shown in Section IV-C.

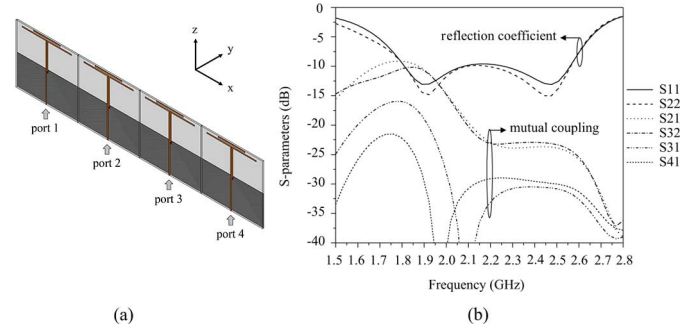


Fig. 4. Four-element linear phased array using quasi-Yagi antennas in collinear configuration. (a) Collinear configuration. (b) Reflection coefficient and mutual coupling values.

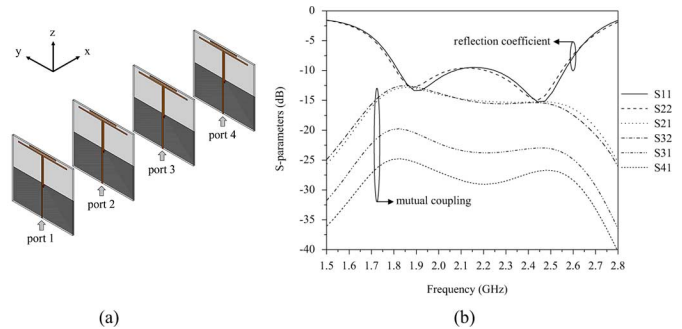


Fig. 5. Four-element linear phased array using quasi-Yagi antennas in side-by-side configuration. (a) Side-by-side configuration. (b) Reflection coefficient and mutual coupling values.

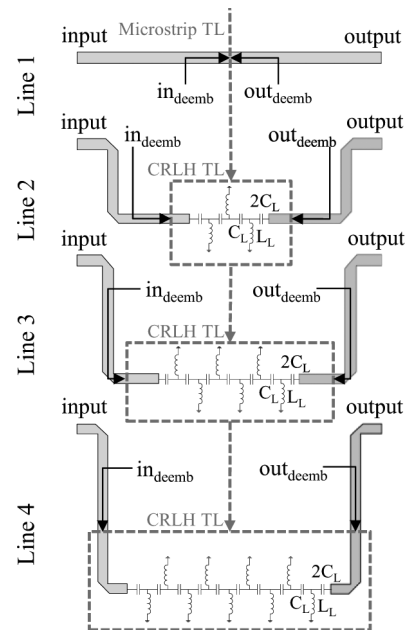


Fig. 6. Illustrative layout of the feed lines for four-element phased array.

IV. IMPLEMENTATION OF CRLH-BASED PHASED ARRAY

When the CRLH lines are combined with proper power dividers, a more versatile frequency-scanning phased-array feed network can be designed. As noted in Section III, the phase component is mainly dictated by the dispersive CRLH lines. On the other hand, amplitude distribution can be controlled by

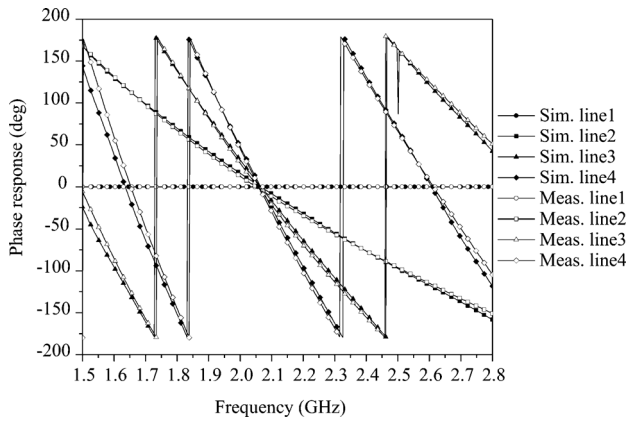


Fig. 7. Simulated and measured phase response of CRLH dispersive lines only.

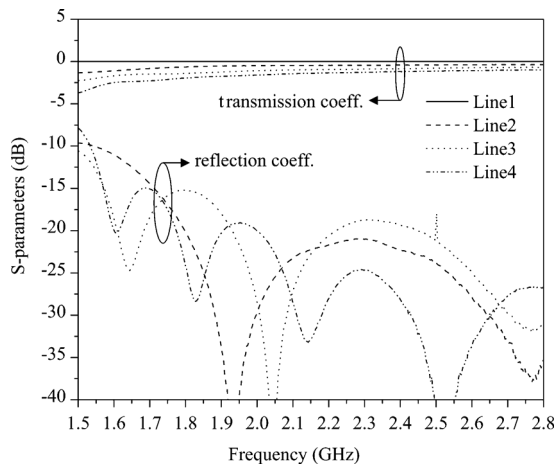


Fig. 8. Measured transmission coefficients and reflection coefficients of CRLH dispersive lines only.

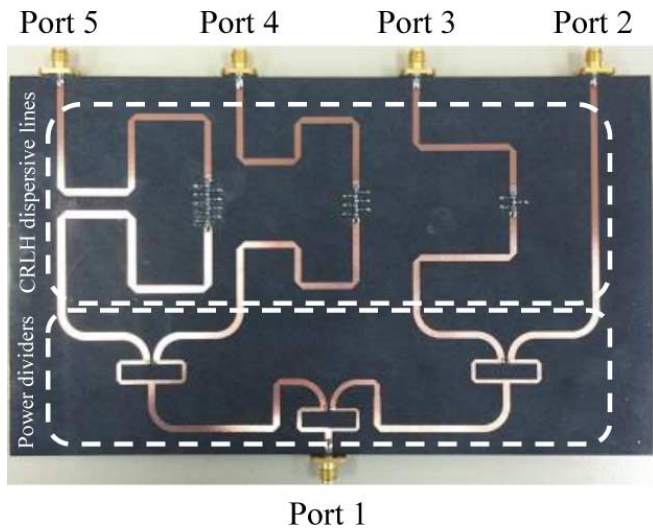


Fig. 9. Photograph of the fabricated linear 1-D phased-array feed network based on CRLH Tls with uniform amplitude distribution.

the power dividers and radiated polarization properties depend purely on the antenna elements used along with the proposed network. Therefore, independent design freedom is allowed by simply selecting and combining the independent functional

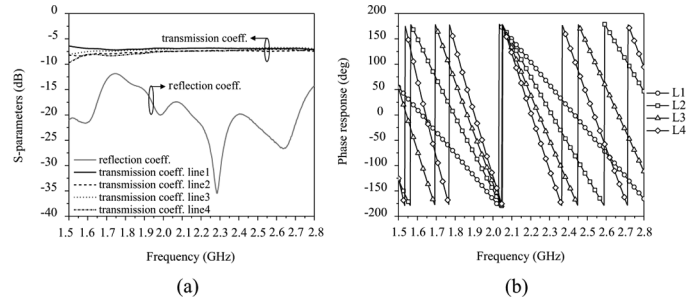


Fig. 10. Measured: (a) *S*-parameters and (b) phase response of CRLH phased-array feed network with uniform amplitude distribution.

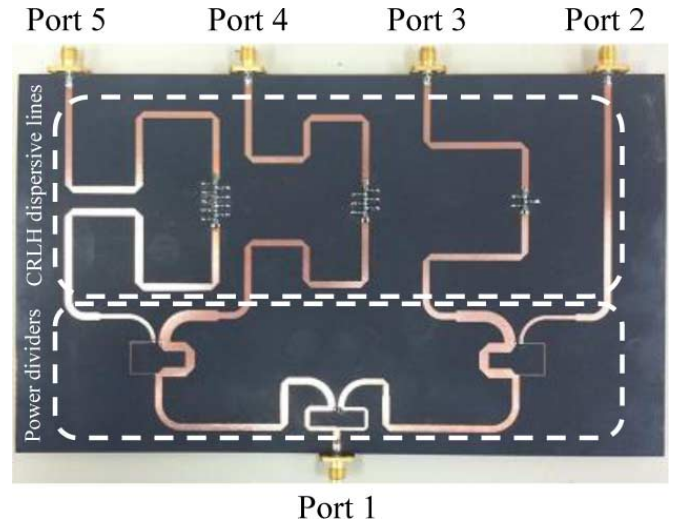


Fig. 11. Photograph of the fabricated linear 1-D phased-array feed network based on CRLH Tls with tapered amplitude distribution.

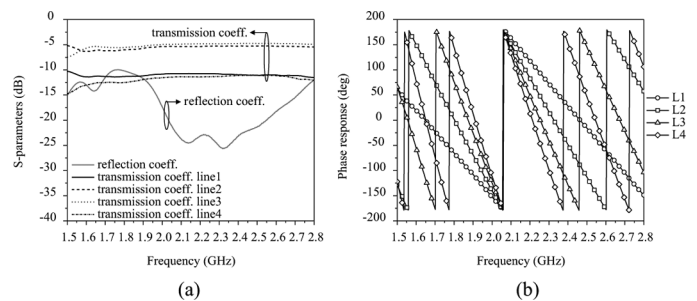


Fig. 12. Measured: (a) *S*-parameters and (b) phase response of CRLH phased-array feed network with tapered amplitude distribution.

blocks (power divider, dispersive feed lines, and antenna elements) to meet most design specifications, such as the type and orientation of the radiated polarization, cross-polarization levels, main-lobe level to SLL, and frequency-scanning range. In the following sections, two sets of frequency-scanning phased-array feed networks based on CRLH dispersive lines are designed using quasi-Yagi antennas to demonstrate the versatility and simplicity in designing and controlling the radiated properties of the antenna array. First, a CRLH array feed network is designed to provide uniform amplitude distribution for maximum directivity, and the second network is fed with tapered amplitude distribution to examine the SLL controllability of the radiated pattern. Also, for each feed network,

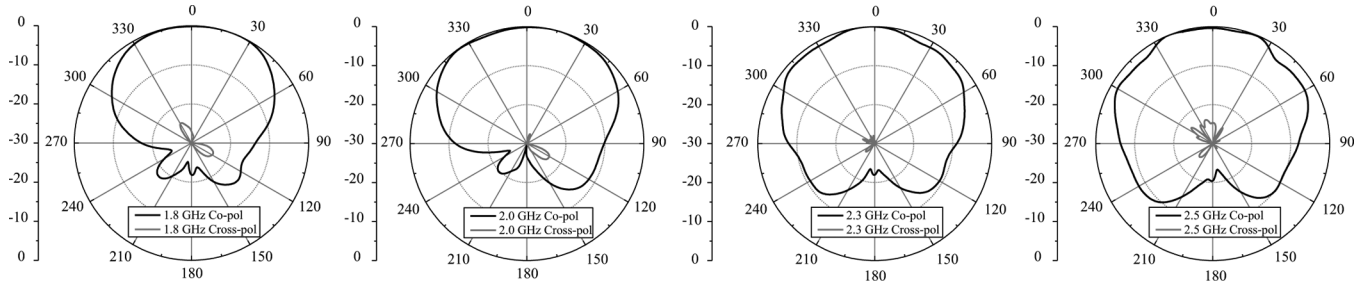


Fig. 13. Measured normalized E -plane co-pol (black) and cross-pol (gray) patterns in decibel scale for frequencies: 1.8, 2.0, 2.3, and 2.5 GHz.

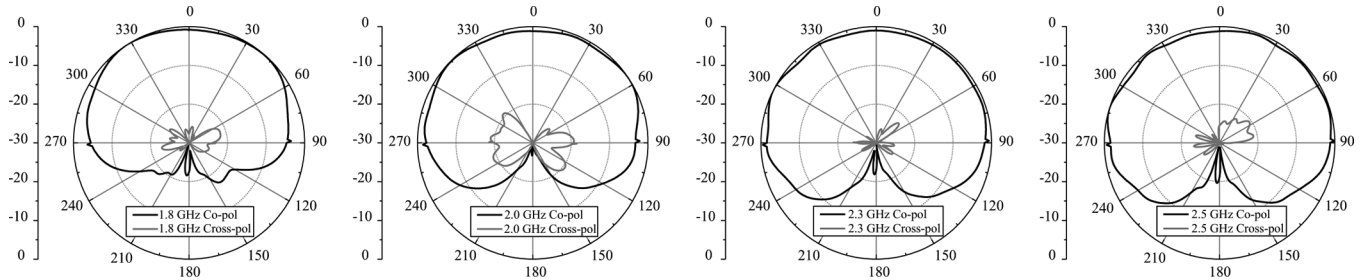


Fig. 14. Measured normalized H -plane co-pol (black) and cross-pol (gray) patterns in decibel scale for frequencies: 1.8, 2.0, 2.3, and 2.5 GHz.

quasi-Yagi antennas are oriented to collinear and side-by-side configurations to show simple polarization controllability of the array system.

A. Wideband Quasi-Yagi Antenna

Quasi-Yagi antennas have been extensively studied both as a single element and in an array. In both cases, these linearly polarized antennas provide good polarization selectivity, can be designed electrically small, provide directive radiation beam pattern, and offer sufficient bandwidth needed for the frequency-scanning operation [16]–[18]. Both simulated and measured results show reflection coefficient values below -10 dB throughout the operating band: $\omega = 1.8$ to 2.5 GHz (Fig. 3). When starting the phased-array network design, inter-element spacing needs to be carefully determined for a given antenna element to satisfy both maximum tolerable mutual coupling levels between the antennas and to avoid the onset of the grating lobe [19]. Generally the inter-element spacing is set to

$$d_{\max} < \frac{\lambda}{1 + |\sin \theta_o|}. \quad (6)$$

However, undesired mutual coupling between the antenna elements at the lower frequencies will limit close placement. Prior to finalizing the inter-element spacing, a mutual coupling study is carried out using full-wave simulation to ensure the levels are kept under reasonable value. In the proposed design, inter-element spacing of $d = 64$ mm ($\approx 0.4 \times \lambda_{0.1}$ and $\approx 0.5 \times \lambda_{0.2}$) is used. In both collinear and side-by-side four-element linear array configuration, reflection coefficient and mutual coupling levels are maintained below -10 dB, as shown in Figs. 4 and 5. Extra optimization may further enhance both levels.

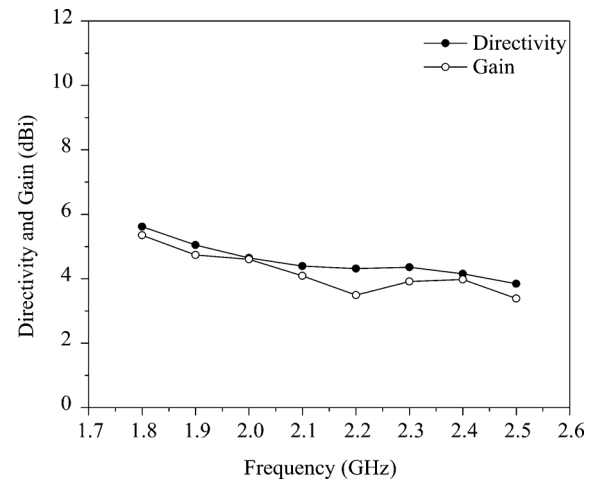


Fig. 15. Measured directivity and gain of the quasi-Yagi antenna.

B. CRLH-Based Phase Advance/Delay Lines For Frequency-Scanning Phased-Array Network

Once the inter-element value is determined, required phase values can be calculated to direct the main beam toward the desired directions. A detailed systematic design guide of CRLH feed lines are explained in [20]. Although the design guides are geared toward designing dual-band phased array, the same procedure also applies to the frequency-scanning phased array. The required relative phase values at the two end frequencies for the desired main beam angles can be obtained based on the array theory as follows:

$$\alpha_{\omega_1/\omega_2} = -k_{\omega_1/\omega_2} d \sin \theta_{o-\omega_1/\omega_2}. \quad (7)$$

For demonstrational purpose, the CRLH feed networks are designed to scan from $\theta_o = -30^\circ$ to $+30^\circ$ between the fre-

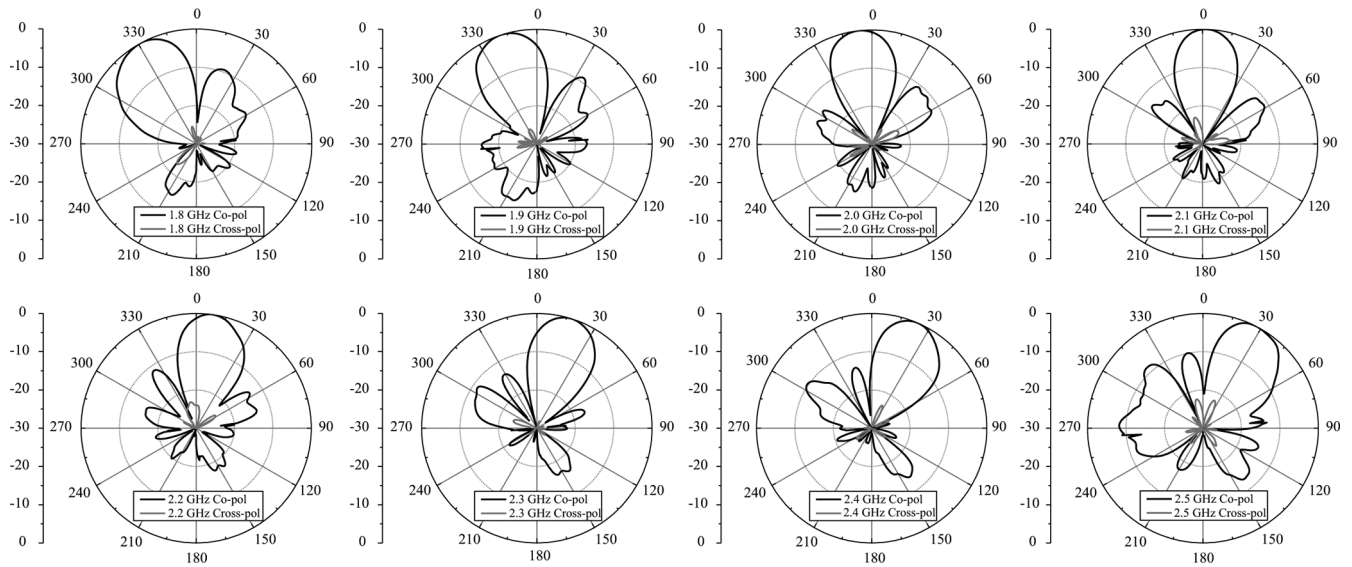


Fig. 16. Measured four-element array normalized E -plane co-pol (black) and cross-pol (gray) radiation patterns in decibel scale for frequencies from 1.8 to 2.5 GHz using uniform amplitude CRLH phased-array feed network in collinear configuration.

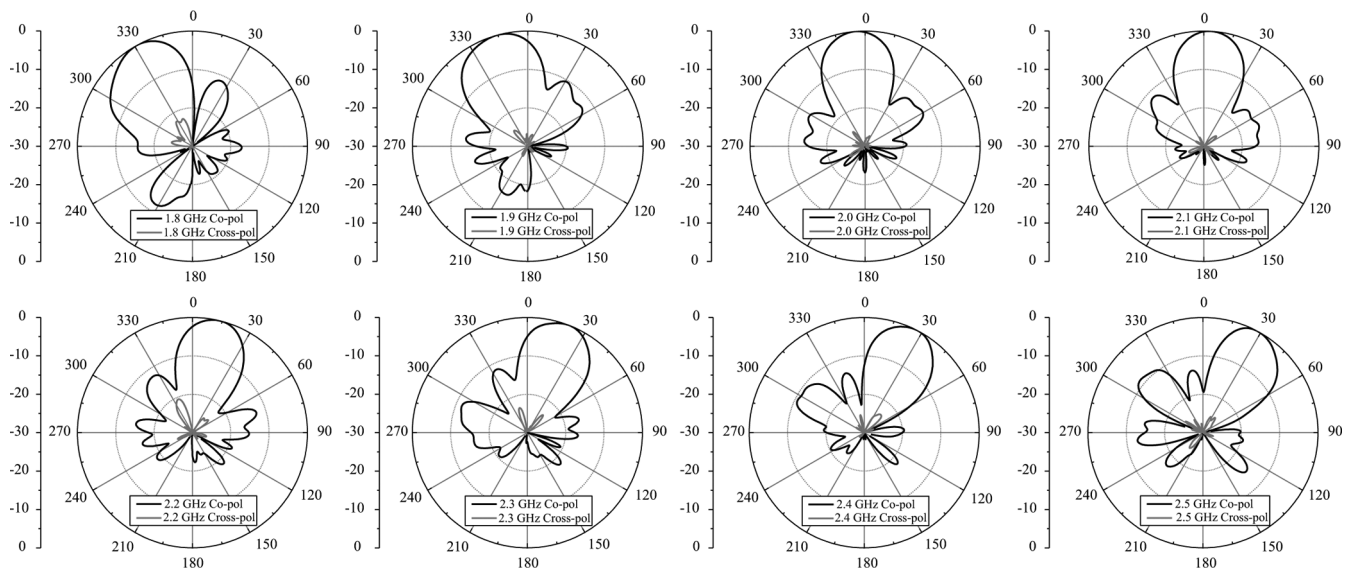


Fig. 17. Measured four-element array normalized H -plane co-pol (black) and cross-pol (gray) radiation patterns in decibel scale for frequencies from 1.8 to 2.5 GHz using uniform amplitude CRLH phased-array feed network in side-by-side configuration.

frequencies $\omega_1 = 1.8$ GHz to $\omega_2 = 2.5$ GHz. Unlike the previous CRLH-based phased-array feed network designs [15] and [20], in order to minimize the number of the total lumped element used, phase reference line (line 1) does not have the CRLH components. Instead, if a conventional microstrip line is used for the first antenna element (Fig. 6), the calculated reactance values of the first CRLH lines (line 2, feeding the second antenna element) using (5) are $L_L = 2.65$ nH, $C_L = 1.06$ pF, $L_R = 5.61$ nH, and $C_R = 2.24$ pF with $n = 3$. Three unit-cells are needed to push the high- and low-pass cutoff frequencies outside the operating frequency band [13]. These ideal reactance values will generate the phase response of $\phi_{-\omega_1} = 69.12^\circ$ and $\phi_{-\omega_2} = -96^\circ$ at the two far-end frequency points ω_1 and ω_2 , thereby directing the main beams to -30° and $+30^\circ$, respectively. For every added antenna element, the same CRLH

sections (in this case, three unit-cells composed of the same reactance values) can be added in a cascaded fashion to ensure the same progressive phase shifting (α) for each operating frequency point within the operating bandwidth. To further reduce the total number of lumped elements and provide better tuning capability, hybrid implementation is used to realize the CRLH lines [13]. RH and LH portions are realized using microstrip lines and lumped elements, respectively. In the final fabricated circuits, $L_L = 3$ nH and $C_L = 1.3$ pF are used, and right-hand microstrip line lengths for each paths are adjusted accordingly to provide the required phase response for the design frequencies (4). The measured phase response of the phase advance/delay lines match well to the desired simulated data (Fig. 7). In both simulated and measured results, the ports are de-embedded to in_{deemb} and $\text{out}_{\text{deemb}}$ positions, as shown in Fig. 6. Once the

phase engineered CRLH dispersive lines are designed, they are combined into two sets of feed networks based on a corporate feeding scheme. One of the circuits uses equal power dividers to provide uniform amplitude distribution that provides maximum directivity, while the other feed network is designed to provide tapered current amplitude distribution to minimize the SLL.

C. CRLH Feed Network With Uniform Amplitude Distribution

For a given array size and dimension, uniform current amplitude distribution provides the highest directivity owing to the space-angle Fourier relationship [21]. A simple corporate feeding network can be used to provide uniform amplitude distribution. As mentioned in Section IV-B, a longer CRLH path introduces more loss, thereby creating amplitude imbalance at the output ports of the feed network. This result is shown in Fig. 8, where larger insertion losses are produced for longer CRLH lines. Measured results show around 0.2-dB loss per CRLH unit-cell. This loss may be reduced using high $-Q$ lumped elements, but it cannot be completely eliminated. However, the amplitude imbalance can be minimized by adding an unequal power divider at the first power division stage. Using a 1-dB power divider, the power imbalance is reduced from 2 to 1 dB and 1 to 0 dB at ω_1 and ω_2 , respectively. The fabricated uniform amplitude CRLH-based phased-array network is shown in Fig. 9. Simulated and measured S -parameters and phase-response plots are shown in Fig. 10. Meandered lines are used to efficiently use the substrate area and miniaturize the overall circuit dimension. The entire circuit is fabricated on Rogers RT/Duroid 5880 ($\epsilon_r = 2.2$, $h = 31$ mil) substrates.

D. CRLH Feed Network With Tapered Amplitude Distribution

Although uniform amplitude distribution provides the highest directivity, it suffers from undesired larger SLL. To reduce the SLL, tapered amplitude may be used. Theoretically, binomial distribution may be used to completely eliminate the sidelobes; however, it requires a relatively more drastic amplitude tapering requirement. For a four-element equally spaced linear array, the binomial current amplitude distribution of 1:3:3:1 (power distribution of 1:9:9:1) is needed to obtain the minimum SLL. Although binomial distribution is achievable, to relax design and fabrication complexity, Dolph–Chebyshev distribution is selected. Sidelobes are not completely eliminated, but SLL can be suppressed below the pre-specified level. Standard Dolph–Chebyshev synthesis with a four-element equally spaced linear array for SLL of -26 dB requires current amplitude distribution of 1:2.13:2.13:1 [22]. To ease both the design procedure and fabrication process, a Wilkinson power divider is designed to provide current amplitude distribution of 1:2:2:1 (power distribution of 1:4:4:1) [23], [24]. The fabricated tapered amplitude CRLH-based phased-array network is shown in Fig. 11. Simulated and measured S -parameters and phase-response plots are shown in Fig. 12. Adding a 4:1 divider in the second stage shows excellent matching and desired dividing ratio of 6 dB between the inner (ports 3 and 4) and outer (ports 2 and 5) ports.

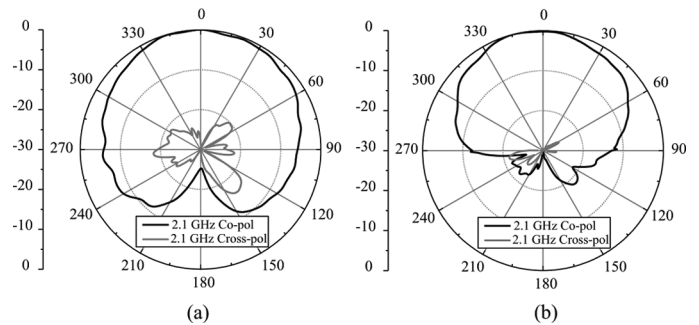


Fig. 18. Measured four-element array normalized co-pol (black) and cross-pol (gray) radiation patterns in decibel scale for frequency = 2.1 GHz using uniform amplitude CRLH phased-array feed network for: (a) collinear (H -plane) and (b) side-by-side configuration (E -plane).

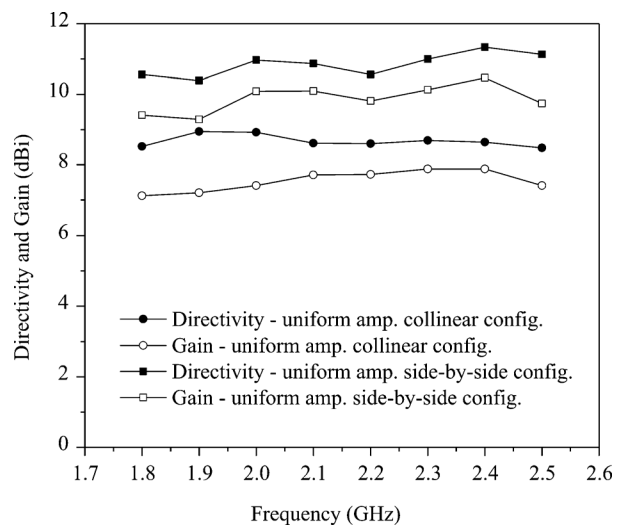


Fig. 19. Measured directivity and gain of uniform amplitude CRLH phased array.

V. RADIATION PATTERNS: MEASUREMENT SETUP AND RESULTS

A. Radiated Measurement Setup

Radiation patterns and directivity for quasi-Yagi antennas and phased-array antennas using both a uniform amplitude and tapered amplitude CRLH phased-array network are measured in the near-field chamber with a WR-430 waveguide probe. The radiated gain values for each circuit are computed based on the gain comparison method using a standard gain horn antenna with a gain of 16 dBi.

B. Measured Results For Quasi-Yagi Antenna Only

The quasi-Yagi antenna has a quasi-dipole radiation pattern that resembles a doughnut-shaped radiation pattern. However, the ground plane on the backside acts as a reflector to enhance the directivity toward the opposite direction. Co-pol and cross-pol radiation patterns for both E - and H -plane radiation patterns are shown in Figs. 13 and 14, respectively. Measured directivity and gain plots are shown in Fig. 15.

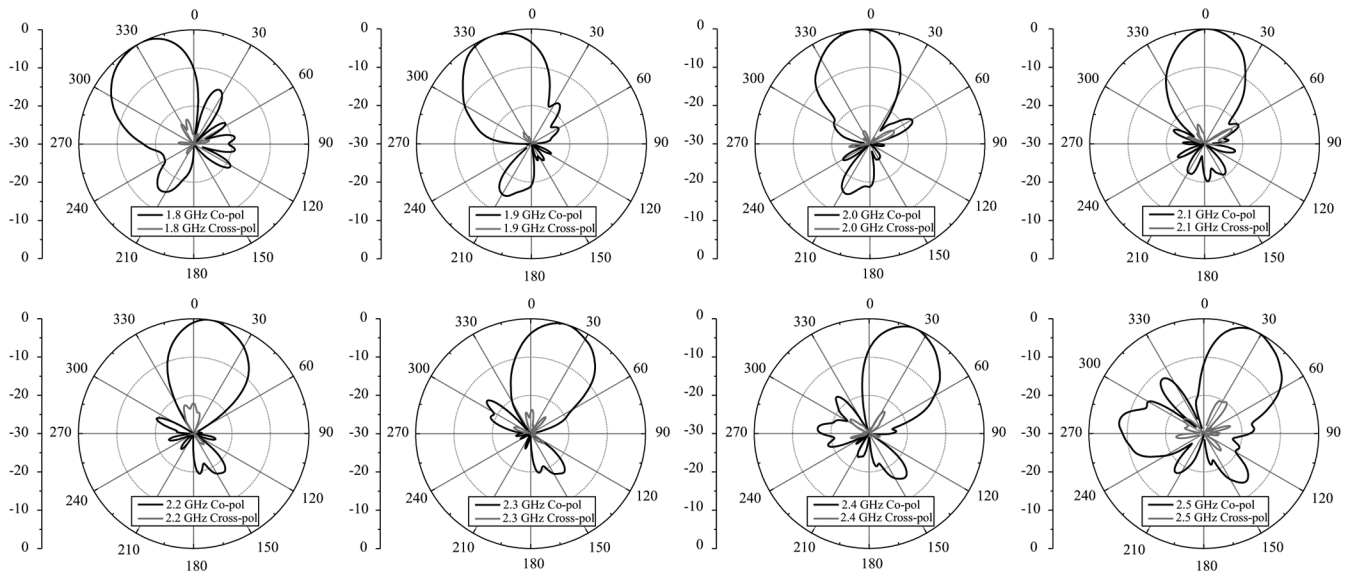


Fig. 20. Measured four-element array normalized E -plane co-pol (black) and cross-pol (gray) radiation patterns in decibel scale for frequencies from 1.8 to 2.5 GHz using tapered amplitude CRLH phased-array feed network in collinear configuration.

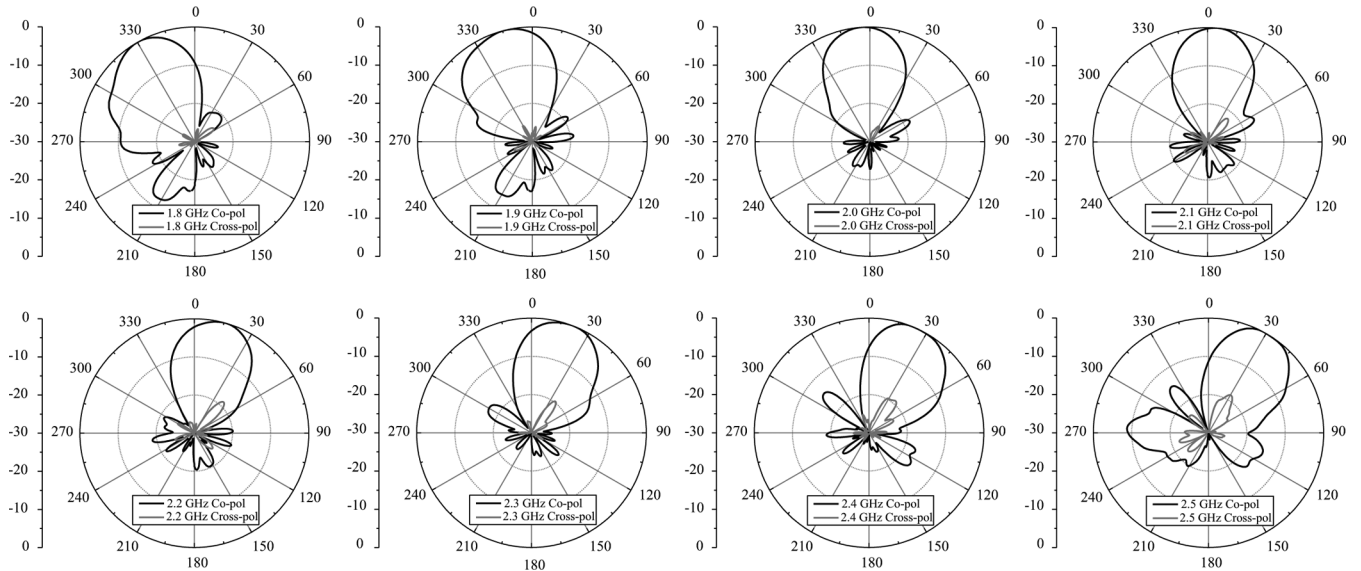


Fig. 21. Measured four-element array normalized H -plane co-pol (black) and cross-pol (gray) radiation patterns in decibel scale for frequencies from 1.8 to 2.5 GHz using tapered amplitude CRLH phased-array feed network in side-by-side configuration.

C. Measured Results Using CRLH Feed Network With Uniform Amplitude Distribution

The measured radiation patterns for both antenna orientations using uniform amplitude distribution show good polarization properties with the scan directions that match well to the designed angles. Measured main beam angles for collinear configuration along the scan angle are $\theta_o = -29^\circ$ and $\theta_o = +28^\circ$ for ω_1 and ω_2 , respectively (Fig. 16). For side-by-side configuration, the measured main beam angles steered to $\theta_o = -29^\circ$ and $\theta_o = +28^\circ$ for ω_1 and ω_2 , respectively (Fig. 17). The E -field is oriented parallel to the scanning angle in the collinear configuration and the E -plane is orthogonally oriented in the side-by-side configuration. The SLL is around 10 dB below the main lobe. The cross-pol level is below 20 dB throughout the entire scan frequency for both E -plane and H -plane patterns. Similar to the

CRLH LWAs, a fan-beam radiation pattern is generated. However, the beamwidth in the plane orthogonal to the array scanning direction may also be controlled by selecting antennas that are electrically long or orienting the antenna to align the element pattern null location along the y -direction, similar to the orientation shown in Fig. 5(a). For a quasi-Yagi antenna, the narrower beamwidth can be observed when the array is arranged in a side-by-side configuration (Fig. 18). Measured directivity and gain values are shown in Fig. 19. Compared to the tapered amplitude case, a uniform amplitude CRLH phased-array antenna shows more of a directive radiation pattern.

D. Measured Results Using CRLH Feed Network With Tapered Amplitude Distribution

Although the main beam width is wider than that of the equal amplitude case, the SLL are much reduced in the tapered ampli-

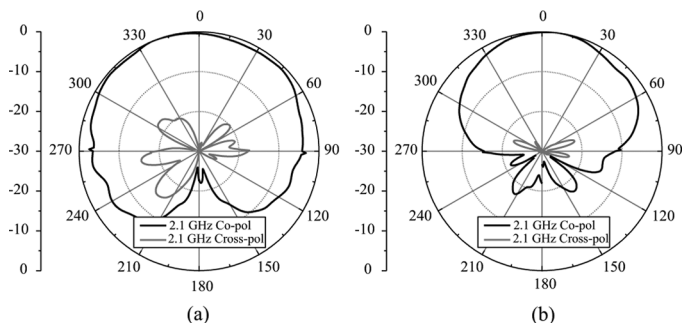


Fig. 22. Measured four-element array normalized co-pol (black) and cross-pol (gray) radiation patterns in decibel scale for frequency = 2.1 GHz using tapered amplitude CRLH phased-array feed network for: (a) collinear (H -plane) and (b) side-by-side configuration (E -plane).

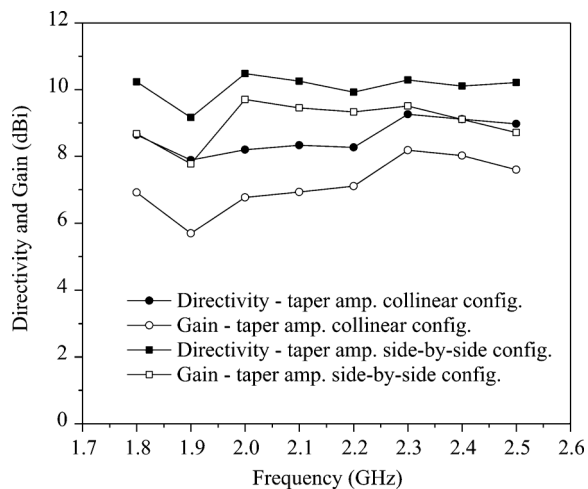


Fig. 23. Measured directivity and gain of tapered amplitude CRLH phased array.

tude case. The SLL is below 20 dB near the center frequency, but tend to be relaxed as the frequency shifts away from the designed center frequency. Early onset of the grating lobe shown at $\omega = 2.5$ GHz in Figs. 20 and 21 is due to widening of the main lobe (in the AF universal pattern) resulting from tapered amplitude distribution. If desired, this grating lobe may be eliminated by placing the antenna elements closer to each other. Similar to the uniform amplitude case, the cross-pol level is suppressed below 20 dB throughout the scan frequency. Measured main beam angles for collinear configuration are $\theta_o = -28^\circ$ and $\theta_o = +27^\circ$ for ω_1 and ω_2 , respectively. For the side-by-side configuration, the measured main beam angles are $\theta_o = -30^\circ$ and $\theta_o = +29^\circ$ for ω_1 and ω_2 , respectively. The beamwidth in Fig. 22 is also narrower for the side-by-side configurations. Measured directivity and gain values are shown in Fig. 23.

VI. CONCLUSION

An all-passive frequency-scanning phased array based on the CRLH feed network provides versatile design freedom that allows easy controllability of radiated parameters including: polarization type, polarization orientation, cross-pol level, directivity, and SLL. The entire circuit can be built using passive components on planar substrates. It can direct the main beam toward the desired elevation angles while allowing bidirectional

operation. A simple systematic design approach provides excellent measurement results that match well with the predicted values. The proposed CRLH phased-array network may also be used with any off-the-shelf wideband antennas. Although this method will not replace the CRLH LWA, it may provide benefits for other applications that require more sensitive control of the frequency-scanning antenna radiation patterns.

ACKNOWLEDGMENT

The authors would like to thank J. Kovitz and T. Brockett for their support with the radiated measurement setups.

REFERENCES

- [1] W. Menzel, "A new-traveling wave antenna in microstrip," *Arch. Elektr. Uebertrag. Tech.*, vol. 33, no. 4, pp. 137–140, Apr. 1979.
- [2] A. Oliner and K. Lee, "Microstrip leaky wave strip antenna," in *Proc. IEEE AP-S Int. Symp. Dig.*, Jun. 1986, pp. 443–446.
- [3] C. Caloz and T. Itoh, "Array factor approach of leaky-wave antennas and application to 1-D/2-D composite right/left-handed (CRLH) structures," *IEEE Microw. Wireless Compon. Lett.*, vol. 14, no. 6, pp. 274–276, Jun. 2004.
- [4] L. Lei, C. Caloz, and T. Itoh, "Dominant mode leaky-wave antenna with backfire-to-endfire scanning capability," *Electron. Lett.*, vol. 38, no. 23, pp. 1414–1416, Nov. 2002.
- [5] A. Grbic and G. V. Eleftheriades, "A backward-wave antenna based on negative refractive index $L-C$ networks," in *Proc. IEEE AP-S Int. Symp. Dig.*, Jun. 2002, vol. 4, pp. 340–343.
- [6] M. R. M. Hashemi and T. Itoh, "Coupled composite right/left-handed leaky-wave transmission-lines based on common/differential-mode analysis," *IEEE Trans. Microw. Theory Techn.*, vol. 58, no. 12, pp. 3645–3656, Dec. 2010.
- [7] F. P. Casares-Miranda, C. Camacho-Penalosa, and C. Caloz, "High-gain active composite right/left handed leaky wave antenna," *IEEE Trans. Antennas Propag.*, vol. 54, no. 8, pp. 2292–2300, Aug. 2006.
- [8] Y. Dong and T. Itoh, "Composite right/left-handed substrate integrated waveguide and half mode substrate integrated waveguide leaky-wave substrate," *IEEE Trans. Antennas Propag.*, vol. 59, no. 3, pp. 767–775, Mar. 2011.
- [9] C. Caloz and T. Itoh, *Electromagnetic Metamaterials: Transmission Line Theory and Microwave Applications*. New York, NY, USA: Wiley, 2005.
- [10] C. Caloz, T. Itoh, and A. Rennings, "CRLH metamaterial leaky-wave and resonant antennas," *IEEE Antennas Propag. Mag.*, vol. 50, no. 5, pp. 25–39, Oct. 2008.
- [11] S. Paulotto, P. Baccarelli, F. Frezza, and D. R. Jackson, "Full-wave modal dispersion analysis and broadside optimization for a class of microstrip CRLH leaky-wave antennas," *IEEE Trans. Microw. Theory Techn.*, vol. 56, no. 12, pp. 2826–2837, Dec. 2008.
- [12] I.-H. Lin, M. DeVincentis, C. Carloz, and T. Itoh, "Arbitrary dual-band components using composite right/left-handed transmission lines," *IEEE Trans. Microw. Theory Techn.*, vol. 52, no. 4, pp. 1142–1149, Apr. 2004.
- [13] P. Chi and T. Itoh, "Miniaturized dual-band directional couplers using composite right/left-handed transmission structures and their applications in beam pattern diversity systems," *IEEE Trans. Microw. Theory Techn.*, vol. 57, no. 5, pp. 1207–1215, May 2009.
- [14] C.-H. Tseng and T. Itoh, "Dual-band bandpass and bandstop filters using composite right/left-handed metamaterial transmission lines," *IEEE MTT-S Int. Microw. Symp. Dig.*, pp. 931–934, 2006.
- [15] J. Choi, Y. Dong, and T. Itoh, "Composite right/left-handed (CRLH) phased-array feed network for frequency scanning antenna," in *Eur. Microw. Conf.*, Amsterdam, The Netherlands, Oct. 2012, pp. 755–758.
- [16] Y. Qian, W. R. Deal, N. Kaneda, and T. Itoh, "A uniplanar quasi-Yagi antenna with wide bandwidth and low mutual coupling characteristics," in *IEEE AP-S Int. Symp. Dig.*, Orlando, FL, USA, Jul. 1999, vol. 2, pp. 924–927.
- [17] W. R. Deal, N. Kaneda, J. Sor, Y. Qian, and T. Itoh, "A new quasi-Yagi antenna for planar active antenna arrays," *IEEE Trans. Microw. Theory Techn.*, vol. 48, no. 6, pp. 910–918, Jun. 2000.
- [18] C. J. Lee, C. Caloz, K. M. K. H. Leong, S. M. Han, and T. Itoh, "A planar broadband antenna for UWB pulse transmission," in *Proc. 34th Eur. Microw. Conf.*, Oct. 2004, vol. 3, pp. 1329–1331.

- [19] D. Parker and D. Z. Zimmermann, "Phased arrays theory and architectures," *IEEE Trans. Microw. Theory Techn.*, vol. 50, no. 3, pp. 678–687, Mar. 2002.
- [20] J. Choi and T. Itoh, "Dual-band composite right/left-handed (CRLH) phased-array antenna," *IEEE Antennas Wireless Propag. Lett.*, vol. 11, pp. 732–735, 2012.
- [21] W. L. Stutzman and G. A. Thiele, *Antenna Theory and Design*, 2nd ed ed. New York, NY, USA: Wiley, 1998.
- [22] C. A. Balanis, *Antenna Theory*, 2nd ed ed. New York, NY, USA: Wiley, 1997.
- [23] D. M. Pozar, *Microwave Engineering*, 3rd ed ed. Hoboken, NJ, USA: Wiley, 2005.
- [24] H.-R. Ahn and I. Wolff, "General design equations of three-port unequal power-dividers terminated by arbitrary impedances," in *IEEE MTT-S Int. Microw. Symp. Dig.*, Jun. 2000, pp. 1137–1140.



Jun H. Choi (S'12) received the B.S. degree in electrical engineering from the University of California at Irvine, Irvine, CA, USA, in 2003, the M.S. degree in electrical engineering from the University of California at Los Angeles (UCLA), Los Angeles, CA, USA, in 2007, and is currently working toward the Ph.D. degree in electrical engineering at UCLA.

His research interests include phased-array systems, microwave/millimeter-wave circuit designs, and devices based on CRLH and metamaterial structures.



Jim S. Sun (S'08) received the B.S. degree from National Taiwan University, Taipei, Taiwan, in 2006, the M.S. degree from the University of California Los Angeles (UCLA), Los Angeles, CA, USA, in 2008, and is currently working toward the Ph.D. degree at UCLA.

Since 2007, he has been a Graduate Student Researcher with the Microwave Electronics Laboratory, UCLA. His research activity includes conformal retro-directive arrays in the M.S. program, and tunable filters, directional filters, CRLH TLs, and

antenna design in the Ph.D. program.



Tatsuo Itoh (S'69–M'69–SM'74–F'82–LF'06) received the Ph.D. degree in electrical engineering from the University of Illinois at Urbana-Champaign, Urbana, IL, USA, in 1969.

After a period spent with the University of Illinois, SRI, and the University of Kentucky, he joined the faculty of The University of Texas at Austin, Austin, TX, USA, in 1978, where he became a Professor of electrical engineering in 1981. In September 1983, he was selected to hold the Hayden Head Centennial Professorship of Engineering with The University of

Texas. In January 1991, he joined the University of California at Los Angeles (UCLA), Los Angeles, CA, USA, as Professor of electrical engineering and Holder of the TRW Endowed Chair in Microwave and Millimeter Wave Electronics (currently the Northrop Grumman Endowed Chair). He has authored or coauthored 400 journal publications and 820 refereed conference presentations. He has authored or coauthored 48 books/book chapters in the area of microwaves, millimeter waves, antennas, and numerical electromagnetics. He has generated 73 Ph.D. students.

Dr. Itoh is a member of the Institute of Electronics and Communication Engineers, Japan, and Commissions B and D of USNC/URSI. He was the editor-in-chief of the *IEEE TRANSACTIONS ON MICROWAVE THEORY AND TECHNIQUES* (1983–1985). He was president of the IEEE Microwave Theory and Techniques Society (IEEE MTT-S) (1990). He was the editor-in-chief of *IEEE MICROWAVE AND GUIDED WAVE LETTERS* (1991–1994). He was the chairman of Commission D, International URSI (1993–1996) and Commission D, International URSI (1993–1996). He serves on advisory boards and committees of numerous organizations. He was a Distinguished Microwave Lecturer on Microwave Applications of Metamaterial Structures for the IEEE MTT-S (2004–2006). He was elected a member of the National Academy of Engineering in 2003. He was the recipient of numerous awards, including the IEEE Third Millennium Medal (2000), the IEEE MTT-S Distinguished Educator Award (2000), and the IEEE MTT-S Microwave Career Award (2011).